

Dynamics of a Vibration-Driven One-way Moving Wheeled Robot

Ivan A. Loukanov¹, Venko G. Vitliemov², Ivelin V. Ivanov²

¹University of Botswana, Gaborone, Botswana,

²Ruse University, Ruse, Bulgaria

Abstract: This paper deals with the dynamics of a vibration-driven unidirectionally moving wheeled robot. A dynamic model of the robot is proposed and the equations governing the motion are derived. The conditions for one-way motion of the robot are likewise obtained. Furthermore the conditions for the motion of the wheels with no slippage are also stated. Numerical experiment with the dynamic model of the robot assumed to have linear elastic and dissipative characteristics is conducted and the results obtained are visualized by means of 2D and 3D graphs. The variation of mechanical parameters of the robot on its dynamics are investigated and analyzed. It is found that the mean velocity of the robot is sensitive to the parameters of the mechanical system, mainly: the resonance frequency of the propulsion mechanism, the stiffness and the amount of damping in the system, the coefficient of friction between the wheels and the ground, the initial value of the phase angle of contra-rotating unbalanced masses and the rest of the system parameters. A dynamic intensity criterion is introduced as a measure of the overload of the propulsion mechanism. It is found that low frequency resonance regimes generate smaller dynamic intensity and therefore reduced dynamic load.

Keywords: Wheeled robots, dynamic model, vibration drive, mean velocity of motion, dynamic intensity.

I. Introduction

Mobile robots with vibration-propulsion, known also as vibration-driven robots or vibrobots are subject of increased interest, motivated by their advantages when working under unusual conditions, combined with increased requirements for energy efficiency, tiny size, environmental conditions and human safety. The vibration-driven robot have a simple design because it does not have any driving mechanisms such as gearboxes, prop shafts, differential etc. like in the contemporary vehicles. In the case of the wheeled robot investigated in this study the motion is achieved by the action of inertia forces generated from the periodic motion of synchronized unbalanced contra-rotating masses. The driving mechanism is an oscillating single-degree-of-freedom mechanical system, which operates in close proximity of the main resonance. This determines the appearance of nonlinear dynamic phenomenon's that makes it difficult to study these systems. Most of the studies conducted on vibration-driven robots are related to analytical modeling, testing prototypes and computer simulation of their dynamic behavior [1], [2], [3], [4].

In this study the dynamic model of a one-way moving wheeled robot is investigated based on the experimental data obtained in [5] for a prototype wheeled robot studied in [6] and [7].

II. Dynamic Model

In Fig. 1 and Fig. 2 the physical and the dynamic model of the real prototype of a wheeled robot is presented. It is assumed that all bodies of the mechanical system are shown as plane figures moving in a vertical plane coinciding with the XOZ -plane of the absolute coordinate system $OXYZ$.

The mechanical system of the robot obeys a dynamic symmetry in the direction of the axis OY . This assumption is correct for the propulsion action of the two contra-rotating unbalanced masses $m_3/2$ and for the symmetrically located elastic and dissipative ties, but it is approximate in terms of locations of the centers of gravity of the respective bodies of the system.

The bodies 1 and 2 shown in Fig. 2 having weights G_1 and G_2 respectively are involved in a rectilinear translation motion. The excitation propulsion action of the inertia force, generated by the contra-rotating unbalanced masses $m_3/2$ is directed towards the OX axis. It is defined by the periodic motion of body 3 in respect to body 2, the former considered as a mass point of weight $G_3 = m_3g$. It is moving according to a known periodic harmonic law of motion - $\eta(t)$ as a result of the rotating unbalanced masses.

We introduce three generalized coordinates x_1, x_2, x_3 (Fig. 2), which specify the position of bodies 1, 2 and 3 with respect to the absolute coordinate system $OXYZ$. The coordinates x_1, x_2 and x_3 are related through the equations:

$$\begin{aligned}x_2(t) &= x_1(t) + l_0 + \xi(t), \\x_3(t) &= x_2(t) + l_2 + \eta(t),\end{aligned}\tag{1}$$

where: $\eta(t) = \rho \sin(\omega t + \phi_0)$ is the periodic harmonic law of oscillation of body 3 (the unbalanced masses) with ρ being the amplitude, ω the angular frequency of rotation and ϕ_0 the initial phase angle; Also the distance - l_0 is the original static length of the equivalent spring and l_2 is the distance specifying the position of the center of rotation of the unbalanced masses. All these distances are constants and are measured from the prototype robot shown in Fig. 1 where ξ - is the value of variation of the length of the equivalent spring as compared to its initial static length. The stiffness of equivalent spring is the sum of stiffness of individual springs in the propulsion mechanism since they are connected in parallel between bodies 1 and 3 as shown in Fig. 1.

The wheels 4 and 5 of the robot, performing general plane motion, are considered solid bodies equal in pairs in terms of their masses and are of same diameters. Their mass centers (axes of rotation) have the same forward velocity $V_1 \equiv dx_1/dt$ as that of body 1, since the wheel axes are fixed to it and therefore involved in the forward translation motion of that body. More importantly, the wheels are furnished with one-way roller bearings designated as number 6 in Fig. 2. Each wheel is furnished with one, one-way bearing. The bearings allow only a forward rotation of the wheels blocking the rotation in the opposite direction. According to the manufacturers of these bearings the time required to block the rotation is about 10^{-6} seconds [8]. This means that an instant blockage of the wheel's rotation is achieved during the opposite action of the propulsion force. The expressions for the absolute accelerations of bodies 1, 2 and 3 are shown below:

$$\begin{aligned} a_1 &\equiv d^2x_1/dt^2 \equiv dV_1/dt, \\ a_2 &\equiv d^2x_2/dt^2 \equiv dV_2/dt, \\ a_3 &\equiv d^2x_3/dt^2 = a_2 + d^2\eta/dt^2 = a_2 - \omega^2\eta, \text{ and} \\ \varepsilon &= a_1/r, \end{aligned} \tag{2}$$

where ε is the angular acceleration of each wheel of radius r , assumed rolling without slipping.

The differential equations of motion are derived by using the principle of Kinetostatics [12]. The system is split into multiple bodies and the free-body diagram of each body is shown schematically in Table 1. The weight forces are G_i , $i = 1, 2, \dots, 5$; the normal and friction reactions are N_j , and T_j , respectively with $j = 1, 2$; the forces of interaction among the bodies R_v , $v = 1, 2, 3$; the resultant spring force F_k ; the damping force F_b ; the inertial forces Φ_l , $l = 1, 2, \dots, 5$ and the moments of inertial forces M_ε^Φ , $\varepsilon = 4, 5$. Here $G_i = m_i g$ are the weights of the individual bodies; $F_k = -k\xi$, with $\xi = x_2 - (x_1 + l_0)$ is the value of the dynamic variation of the equivalent spring force having an initial value $F_k(0) = k(s_0 - l_0)$, with $s_0 \equiv x_2(0)$; $F_b = -b|V_2 - V_1|\sigma$ - is the measure of the equivalent dissipative force F_b , where $\sigma \equiv \text{sign}(V_2 - V_1)$ is the step function of Kronecker; $\Phi_l = -m_l a_l$ and $M_\varepsilon^\Phi = -(m_\varepsilon r/2)a_1$ - are the D'Alambert's inertia forces and the moments of inertial forces respectively.

Table 1 shows the free-body-diagrams of the individual bodies 1, 2, 3 acted upon the active forces, reactions and the forces of interaction between the bodies along with the inertia forces and the moments of inertia forces. According to the principle of D'Alambert's these systems of forces are in balance. Among the forces the unknown are the measures of reactions $R_1, R_2, R_3, P_1, P_2, P_3, P_4, N_1, N_2, T_1, T_2$ and the accelerations a_1, a_2, a_3 referred to the selected positive directions, as well as the distance l_3 . From the conditions of equilibrium the expressions of the required unknown parameters are:

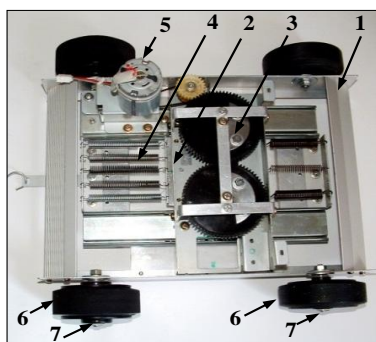


Fig. 1 displays the top view of the prototype robot, where: 1 is the outer frame (body1), 2 - inner frame (body2), 3 contra-rotating eccentric masses (body3), 4 - spring system, 5 - DC motor, 6 - one-way rotating wheels, 7 - one-way rotating bearings.

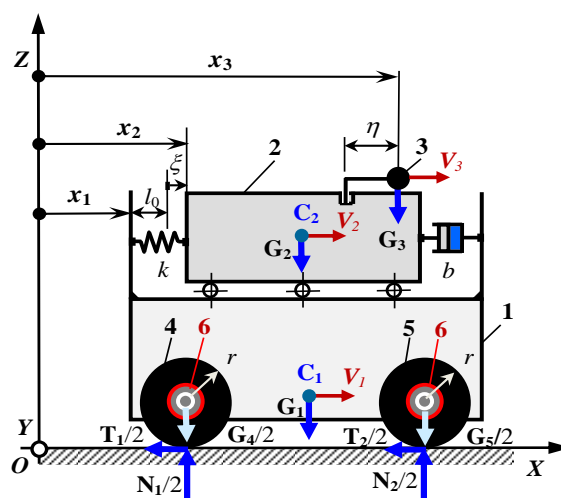


Fig. 2 illustrates the dynamic model of the robot

$$\begin{aligned}
 a_1 &= F_a / [m_1 + (3/2)(m_4 + m_5)], \\
 a_2 &= (m_3 \omega^2 \eta - F_a) / (m_2 + m_3), \\
 a_3 &= a_2 - \omega^2 \eta, \quad R_1 = -m_3 a_3, \quad R_2 = m_3 g, \quad R_3 = (m_2 + m_3) g, \\
 l_3 &= l_1 + \{m_3 [g(l_2 - l_1) - a_3 h_2] - F_a (h_3 - h_1)\} / (m_2 + m_3) g, \quad P_1 = (3/2) m_4 a_1, \\
 P_2 &= \{-F_a h_4 + [(m_2 + m_3) (d_1 - d_3) + m_1 (d_1 - d_2)] g - m_1 a_1 h_5\} / d_1, \quad P_3 = (3/2) m_5 a_1, \\
 P_4 &= \{F_a h_4 + [(m_2 + m_3) d_3 + m_1 d_2] g + m_1 a_1 h_5\} / d_1, \\
 N_1 &= m_4 g + \{-F_a h_4 + [(m_2 + m_3) (d_1 - d_3) + m_1 (d_1 - d_2)] g - m_1 a_1 h_5\} / d_1, \\
 T_1 &= (1/2) m_4 a_1, \quad T_2 = (1/2) m_5 a_1, \\
 N_2 &= m_5 g + \{F_a h_4 + [(m_2 + m_3) d_3 + m_1 d_2] g + m_1 a_1 h_5\} / d_1,
 \end{aligned} \tag{3}$$

where: $F_a = k(x_2 - x_1 - l_0) + b|V_2 - V_1|\sigma$ - combines both the elastic and dissipative forces. Here again $\sigma \equiv \text{sign}(V_2 - V_1)$ is the step function of Kronecker, as explained above.

The differential equations governing the motion of mechanical system and the initial conditions are:

$$\begin{aligned}
 dx_1/dt &= V_1, \quad \text{with initial condition } x_1(t=0) = 0, \\
 dV_1/dt &= [k(x_2 - x_1 - l_0) + b|V_2 - V_1|\sigma] / [m_1 + (3/2)(m_4 + m_5)], \quad \text{with} \\
 \text{initial condition } &V_1(t=0) = 0, \\
 dx_2/dt &= V_2, \quad x_2(t=0) = s_0, \\
 dV_2/dt &= m_3 \omega^2 \rho \sin(\omega t + \phi_0) - [k(x_2 - x_1 - l_0) + b|V_2 - V_1|\sigma] / (m_2 + m_3); \quad V_2(t=0) = 0,
 \end{aligned} \tag{4}$$

And the conditions for simulation of the one-way motion of the robot are:

$$\begin{aligned}
 V_1 &= V_1(t), \quad \text{when } V_1(t) > 0 \quad \text{and} \\
 V_1 &= 0, \quad \text{when } V_1(t) \leq 0.
 \end{aligned} \tag{5}$$

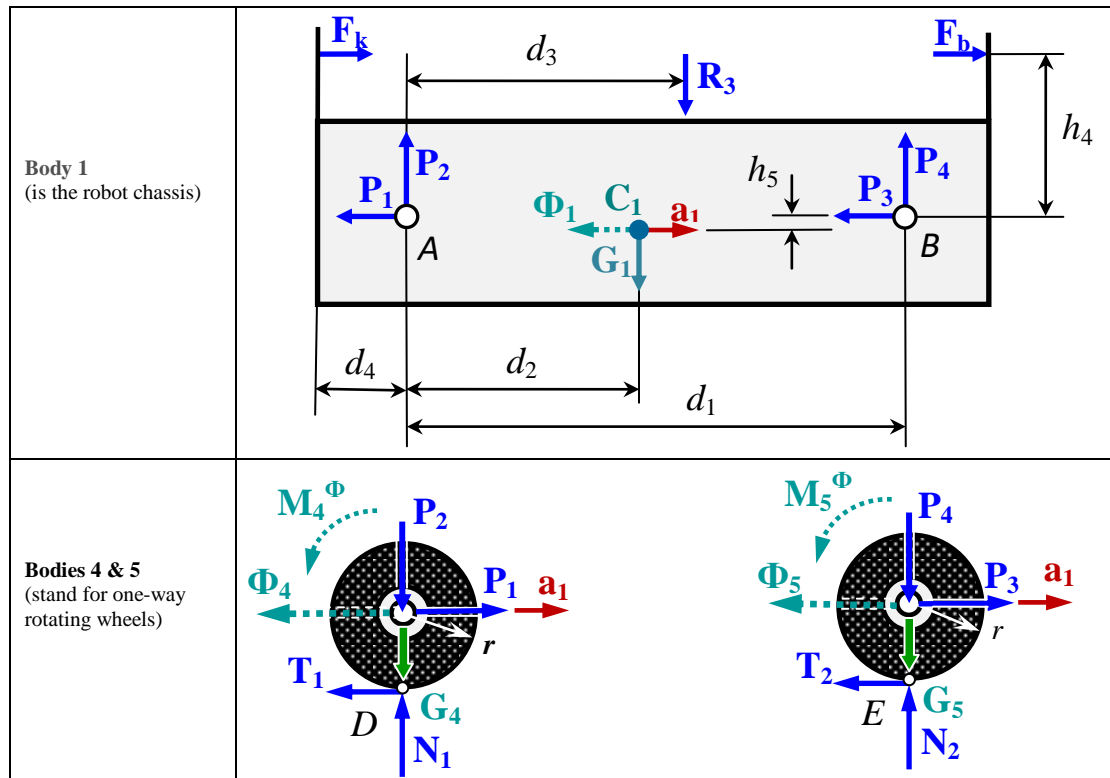
The conditions (5) are realized by means of one-way roller bearings built into the hub of each wheel, allowing a forward rotation of the wheels and preventing the opposite one.

The dynamic model described by equations (3), (4) and (5) has physical meaning if at any instant t the condition for permanent contact between the wheels and the surface is satisfied, such as:

$$\min_t \{N_1(t), N_2(t)\} > 0. \tag{6}$$

Table 1 Free-body diagrams of bodies 1, 2 and 3 with the active, reactive and inertia forces acting on them

Bodies	Free-body diagrams with corresponding forces
<p>Body 3 (stands for the unbalanced counter-rotating masses)</p>	
<p>Body 2 (symbolizes the propulsion mechanism)</p>	



In case that all the wheels are rolling without slipping then the friction forces between them and the contact surface are very small (pure rolling friction) or in the border case they may be equal to the maximum value of the corresponding friction force T_j^* , which is defined as:

$$T_j \leq T_j^* = \mu_0 N, \tag{7}$$

where μ_0 is the static coefficient of friction.

Furthermore, we also assume that under a stabilized motion of the robot the condition (7) is fully satisfied. The mechanical perfection of the robot mechanical system may be assessed by means of various criteria [10]. The major criterion for assessment in kinematic aspects under unidirectional motion of the robot is the mean velocity taken throughout of a specified time interval, given by:

$$\langle V_1 \rangle = \frac{1}{t_f - t_0} \int_{t_0}^{t_f} V_1(t) dt, \tag{8}$$

where $V_1(t)$ satisfies the condition (5).

For the evaluation of the dynamic strength of the robot components when in motion within the time interval $t \in [t_0, t_f]$, the ratio of the mean value of the resultant horizontal propulsion force acting on the wheels to the driving inertia force is used at the time instances $t \in [t_0, t_f]$, $t_0 > 0$ for which $P_1(t) + P_3(t) > 0$ and $R_1(t) > 0$.

As a local criterion for dynamic intensity the ratio $K(t) = F_E(t) / F_D(t)$ of the applied horizontal resultant force on the wheels $F_E(t) = \{P_1(t) + P_3(t)\}^+$ and the driving inertia force $F_D(t) = \{R_1(t)\}^+$ in the instants $t \in [0, t_f]$ for which $P_1(t) + P_3(t) > 0$ and $R_1(t) > 0$ is suggested. Then for the evaluation of dynamic strength of the propulsion system during the stabilized motion of the VibroBot the average value of (9) can be used as a local characteristics for dynamic loading

$$\langle K \rangle = \langle F_E(t) \rangle / \langle F_D(t) \rangle, \tag{9}$$

Where $K(t)$ is valid within the interval $t \in [0, t_f]$.

III. Results of Numerical Experiments

The dynamic model described by equations (1) to (9) allows to simulate the main kinematic and dynamic characteristics of the prototype robot as well as to analyze the effect of variation of mechanical parameters of the model on its dynamic behavior.

Numerical experiment is conducted with the nominal values of parameters of the model involved in equations (3), (4) and (5), obtained from [5] and listed in Table 2. The numerical integration of the differential

equations (4) and (5) within the time interval $t \in [0, t_f]$ is done by using the MATLAB-program *ode113* set with relative accuracy of 10^{-6} and absolute accuracy of 10^{-8} .

Table 2 Prototype parameters obtained from [5] and used for the numerical experiment

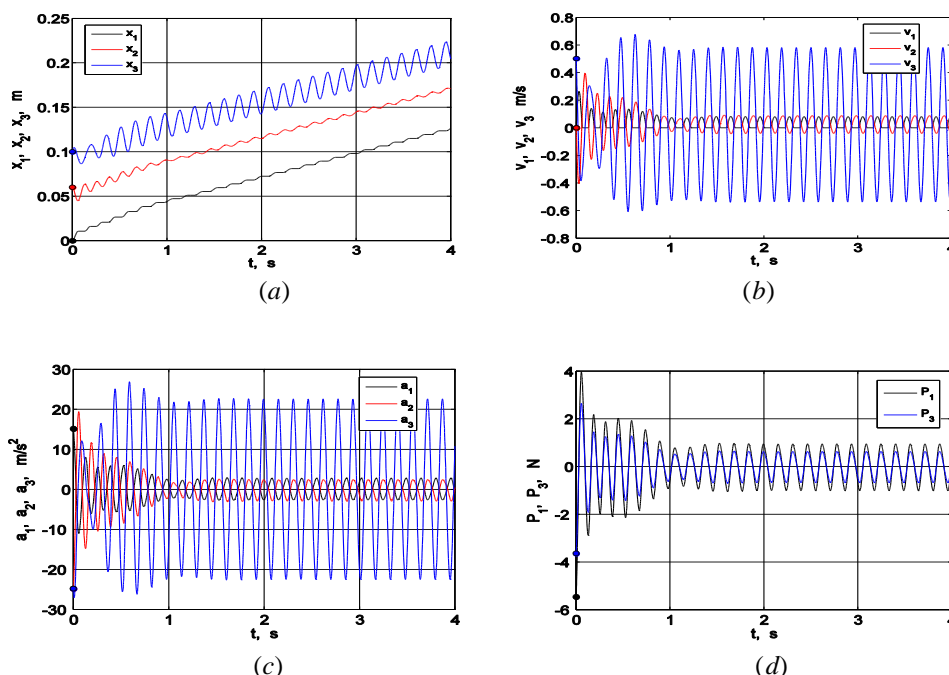
Designations	Values	Units	Designations	Values	Units
l_0	0.045	m	h_5	0.019	m
l_1	0.012	m	ρ	0.0125	m
l_2	0.040	m	R	0.038	m
l_3	Cal-d by Eq.(1)	m	m_1	1.500	kg
$s_0 \equiv x_2(0)$	0.060	m	m_2	1.165	kg
d_1	0.200	m	m_3	0.120	kg
d_2	0.099	m	m_4	0.240	kg
d_3	$d_3 = l_3 + 0.06$	m	m_5	0.160	kg
d_4	0.050	m	ω	40.19	rad/s
h_1	0.035	m	K	2123	N/m
h_2	0.015	m	B	6.215	Ns/m
h_3	0.014	m	φ^0	0	rad
h_4	0.004	m	t_f	4	s

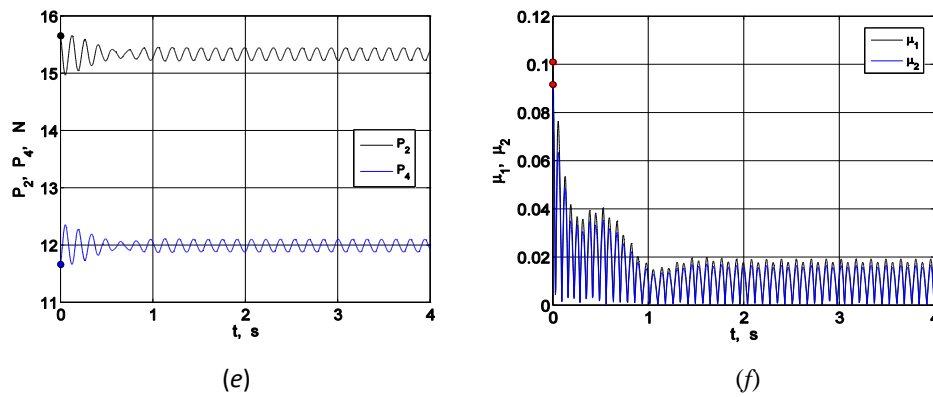
Fig. 3 (a, b, c, d, e, f) illustrate the simulated kinematic characteristics of the robot, which include the displacements, velocities and accelerations of bodies 1, 2, 3 having masses m_1, m_2 и m_3 respectively during their motions. The functions $x_1(t), v_1(t)$ and $a_1(t)$ of the robot have periodic nature of fluctuation, which determine the robot's non-even (vibrating) motion.

The variation of accelerations $a_1(t), a_2(t)$ and $a_3(t)$ is a specific feature of vibration driven robots (Fig. 3c). This makes impossible to achieve uniform change of the acceleration $a_1(t)$. To attain maximum asymmetry of functions $a_3(t)$ and $a_1(t)$ it is possible only by using a program controlled propulsion mechanism as this is the case with the special class of wheeled robots known as Inerzoids, developed and studied by [9].

It is noticed that in Fig, 3d the horizontal forces P_1 and P_3 acting on the wheels bearings are changing in phase, whilst the vertical reactions P_2 and P_4 are varying out of phase Fig. 3 e). It is also seen that the loads on the rear wheels are larger than that of the front ones (Fig. 3 d, e). Likewise with an accuracy of a constant, the components of friction forces of the ground at points D and E of the wheels 4 and 5 are also found variable.

Fig. 3(f) shows the variations of the coefficients of friction $\mu_1 = |T_1(t)/N_1(t)|$ and $\mu_2 = |T_2(t)/N_2(t)|$ as functions of time. The values of these coefficients are considerably lower than the real coefficient of static friction known to be within the range $\mu_0 \in [0.35, 0.75]$. The latter data are experimentally determined by using the prototype robot tested on planes of different materials and surface roughness [7]. Therefore pure rolling of the robot wheels without sliding during the pulsing forward motion of the robot is guaranteed.





Figs. 3(a, b, c, d, e, f) simulated kinematic and dynamic parameters as a function of time

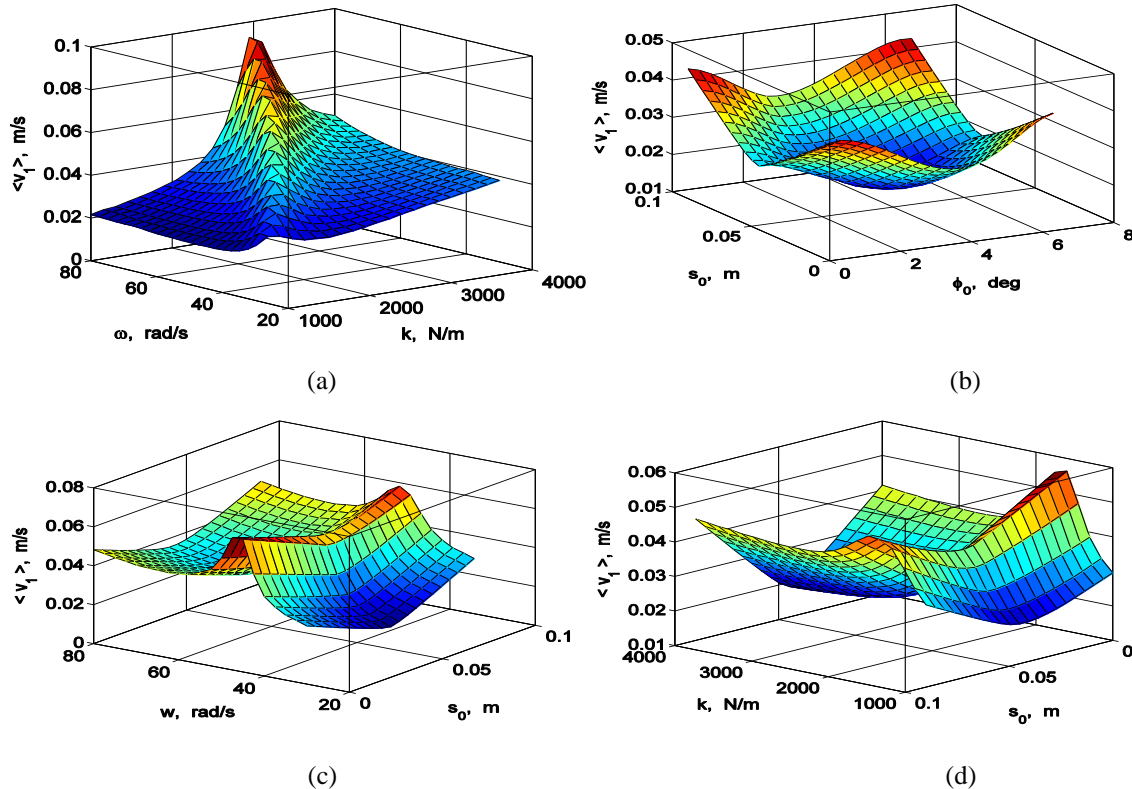
The combined effect of any two parameters of the dynamic model on the mean velocity $\langle V_1 \rangle$ of the robot varying within the intervals $\phi_0 \in [0, 360]^\circ$, $s_0 \in [0, 0.1]$ m, $\omega \in [30, 80]$ rad/s, $b \in [5, 25]$ Ns/m, $k \in [1000, 4000]$ N/m can be seen in Figs. 4 (a, b, c, d, e, f, g, j).

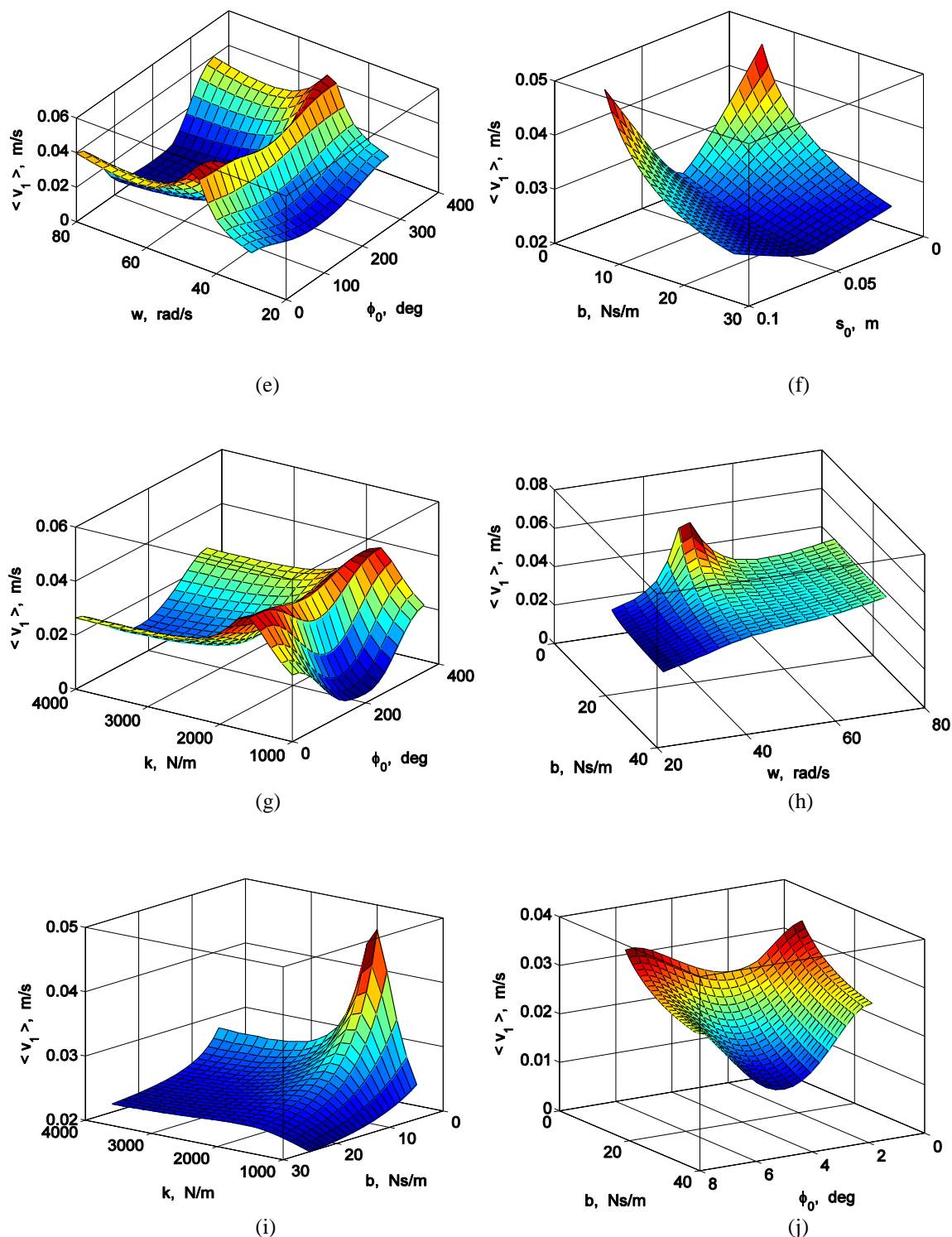
Fig. 4(a) confirms the need for an appropriate selection of the values of parameters ω and k for effective performance of the propulsion mechanism (one-degree-of-freedom oscillating system) within a close proximity of the main resonance. To achieve a fast forward motion of the robot the resonance frequency of the propulsion mechanism should be in the ascending branch of the resonance graph closed to the main resonance.

From Figs. 4(b, c, d, e) we notice that the parameter s_0 - the initial deformation of the equivalent spring has limited effect on the increase of the mean velocity of the robot.

Figs 4(b, f, g, j) illustrate the specific feature of vibration propulsion of the robot that the mean velocity $\langle V_1 \rangle$ is very sensitive to the change of initial phase angle of rotating unbalanced masses ϕ_0 . It is for this reason at the beginning of motion of the robot the value of the starting phase angle must be close to the most-suitable value of $\phi_0 = 0$.

The non-linear character of variation of the function $\langle V_1 \rangle$ reveals the potential opportunity for increasing the mean velocity of the robot by reducing the dissipation of energy in the propulsion mechanism. This can be clearly observed in Figs. 4(h, i, j) where the simulated values of the damping parameter b are small.





Figs. 4 (a, b, c, d, e, f, g, h, i, j) show the variation of mean velocity $\langle V_1 \rangle$ as a function of two parameters

The criterion accounting for the dynamic intensity $\langle K \rangle$ of robot components (9) as a function of parameters ω and k is illustrated in Fig. 5. It is seen that it changes very rapidly with variation of these parameters because they govern the resonance frequency. The larger the stiffness - k of the equivalent spring and the higher the resonance frequency of the propulsion mechanism the greater the dynamic intensity $\langle K \rangle$. Therefore higher dynamic loads are generated in the system and mostly in the one-way bearings contributing to their quick wear and damage. To avoid that problem apparently the factor $\langle K \rangle$ has to be reduced.

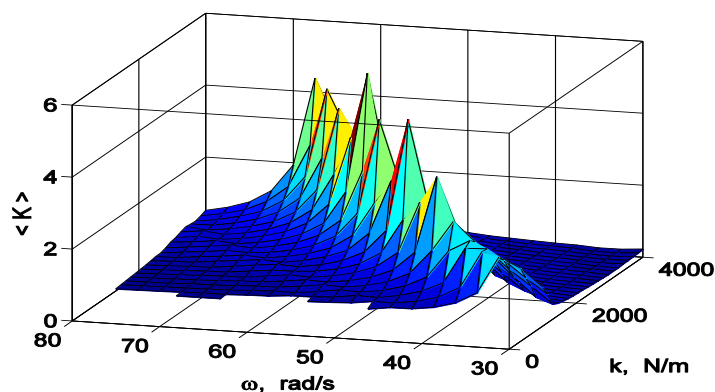


Fig. 5 Variation of dynamic intensity $\langle K \rangle$ as a function of ω and k

Analyzing precisely Fig. 5 it may be concluded that a low frequency resonance creates smaller value of $\langle K \rangle$ hence lower dynamic loading conditions will be generated in mechanical components. Vice versa when a high frequency resonance is set in the propulsion mechanism, mostly between 45-65 Hz, then the peaks of load intensity are getting very high and the possibility of mechanical failure due to overloading rapidly increases. The highest peak of the load intensity $\langle K \rangle$ appears at frequencies of 50-55 Hz. This is mainly due to the bigger inertia forces inducing surface and bending fatigue in the components resulting into intensive wear. It is for this reason a low frequency resonance setup in the propulsion mechanism is recommended. This will generate high resonance amplitudes producing an increased mean velocity leading to reduced accelerations. Therefore low dynamic loads will provide conditions for an increased durability of the propulsion system of the robot.

It is also observed in Fig. 5 that at very high resonance frequencies, above 65 Hz, within the variation of the system parameters, the load intensity drops rapidly owing to the shorter duration of load impulses. Although having high picks these impulses will cause less damage because of the shorter duration of time they act on the components and hence lower wear could be expected in the propulsion system.

IV. Conclusions And Recommendations

The conducted numerical experiment with the dynamic model of the wheeled robot reveals high sensitivity of the mean velocity of motion with respect to the initial pretension s_0 of the equivalent spring, to the initial value of the phase angle ϕ_0 of the periodic rotation motion of unbalanced masses and to the dissipating of energy in the propulsion mechanism. The passive action of the wheels, since they are not subjected to driving torques, ensures pure rolling without sliding over surfaces of different roughness and load carrying abilities. The resonance regime of propulsion appears to be promising approach to achieve a reasonable velocity of motion. On the other hand if the system operates at frequencies (45-65 Hz) it will be subjected to strong dynamic loads and therefore an increased probabilities of fatigue failure of the one-way bearings, the bearings of the contra-rotating masses, the motor bearings as well as the linear bearings guiding the propulsion mechanism should be expected. It was found that low frequency resonance regimes of propulsion cause low dynamic intensity and therefore lesser dynamic loads on the propulsion system. It is for this reason these are preferred as compared to the high resonance settings since they reduce the strength of components and the robot durability.

To prove the theoretical predictions it is recommended conducting durability tests with the prototype robot at different resonance frequencies. Then the endurance limit of the propulsion components and the damage caused should be assessed after certain number of oscillation cycles, or number of revolutions of the contra-rotating masses to find out how the experimental results match the theoretical predictions. Apparently this should be another study to be conducted in determining the life expectancy of the propulsion system. Obviously the life of the propulsion mechanism and that of the one-way bearings will govern the robot durability since these are the main propulsion elements driving the robot in motion.

In conclusion it is recommended that the robot design has to be further improved in order to achieve reversible motion. This would eventually require installing the one-way bearings out of the wheel's hubs and activate them for forward and backward motion separately in a particular manner. That modification would increase ultimately the possible applications of the robot including: In pipe inspection of welded pipes for gas, water and crude oil transportation where the quality of welding is of great importance; Examining underground tunnels and horizontal shafts in the mining industry; Measuring chemical and radiation contaminations in

chemical and nuclear plants; Observing the underground animal habitats in detecting living creatures; For military applications in detecting land mines, unexploded shells, rockets, ammunitions; Also it may be used in the aviation industry for inspecting unreachable spaces where an important equipment need to be checked, etc.

References

- [1] Bolotnik, N., I. Zeidis, K. Zimmermann, S. Yatsun. *Vibration-driven robots*. Presented at the 56th International Scientific Colloquium. Ilmenau University of Technology, Germany, 2011.
- [2] Jatsun, S., N. Bolotnik, K. Zimmerman, I. Zeidis. *Modeling the motion of vibrating robots*. 12-th IFToMM World Congress, Besançon, France, June 18–21, 2007.
- [3] Jatsun, S., V. Dyshenko, A. Yatsun, A. Malchikov. *Modelling of robot's motion driven by the use of vibration of internal masses*. Published in the proceedings of EUCOMES 08 of the Second European Conference on Mechanism Science. M. Ceccarelli (Ed.), Springer, New York, pp. 262–270, 2009.
- [4] Provatidies, C.G. *Design of a propulsion cycle for endless sliding on frictional ground using rotating masses*. Universal Journal of Mechanical Engineering, Vol. 2, No. 2, pp. 35–43, 2014.
- [5] Loukanov, I.A., V.G. Vitliemov, I.V. Ivanov. *Vector identification of forced characteristics of a VibroBot*, sent to EU Journal.
- [6] Loukanov, I.A. *Applications of inertial forces for generating unidirectional motion*. Proceedings of the University of Ruse “Angel Kanchev”, Vol. 53, Book 2, Mechanics, Mechanical and Manufacturing Engineering, pp. 9–19, 2014.
- [7] Loukanov, I.A. *Inertial propulsion of a mobile robot*. IOSR Journal of “Mechanical and Civil Engineering”, Vol. 12, No. 2, Version. 2, pp. 23–33, 2015.
- [8] www.bocabearings.com, one-way Bearings.htm. BOCA Bearing: Miniature bearings for Robotics, Industry & Recreation. Email: info@bocabearings.com
- [9] Tolchin V.N. *Inercoid. Inertia forces as a source of unidirectional motion*. Perm’s Publishing, Perm, 1977 (in Russian).
- [10] Gorskii B. E. *Dynamic enhancements of mechanical systems*, Technical Publishing House, Kiev, 1987 (in Russian)
- [11] Blekhman, I.I. *Vibrational Mechanics: Nonlinear dynamic effects, General approach, Applications*. World Scientific, Singapore, 2000.
- [12] Meriam, J.L., L.G. Kraige. *Engineering Mechanics, Vol. 1, Statics*. John Wiley & Sons, New York, 201.